# A Real-Time Global Sea Surface Temperature Analysis

RICHARD W. REYNOLDS

*Climate Analysis Center, NMC/NWS/NOAA, Washington, DC*

(Manuscript received 7 May 1987, in final form 25 August 1987)

ABSTRACT

A global monthly sea surface temperature analysis is described which uses real-time in situ (ship and buoy) and satellite data. The method combines the advantages of both types of data: the ground truth of in situ data and the improved coverage of satellite data. The technique also effectively eliminates most of the bias differences between the in situ and satellite data. Examples of the method are shown to illustrate these points.

Sea surface temperature (SST) data from quality-controlled drifting buoys are used to develop error statistics for a 24-month period from January 1985 through December 1986. The average rms monthly error is 0.78°C; the modulus of the monthly biases (i.e., the average of the absolute value of the monthly biases) is 0.09°C.

## 1. Introduction

In February 1985 the World Meteorological Organization and the U.S. National Weather Service established a global sea surface temperature (SST) data center at the U.S. National Meteorological Center (NMC) in support of the World Climate Research Program's Tropical Oceans and Global Atmosphere (TOGA) effort. The SST center collects in situ (ship and buoy) and satellite SST measurements in real time and uses these data to produce analyses of monthly mean global SST on a 2-deg latitude–longitude grid for the 10-year TOGA period (1985–94). The activities of NMC in this task are divided between two groups: the Climate Analysis Center, responsible for technical guidance, and the Ocean Products Center, responsible for operations.

The purpose of this paper is to describe the present analysis techniques and to give a preliminary evaluation of their accuracy by use of quality-controlled SST data from drifting buoys.

## 2. SST analyses

Three analyses are produced by NMC: an in situ, a satellite, and a "blended" analysis. All analyses are computed relative to the monthly SST climatology of Reynolds and Roberts (1987) which is discussed at the end of this section.

### *a. The in situ analysis*

The SST data used in the in situ analysis are obtained from the NMC archive of surface marine observations. These data consist of all ship and buoy observations available to NMC on the Global Telecommunication System (GTS) within 10 h of observation time. This archive is accessed daily to extract and save all new SST observations.

The monthly distribution of in situ observations (see Fig. 1) is adequate to describe the SST patterns between 30°S and 60°N except in the central and eastern tropical and South Pacific. However, the individual observations are subject to large errors in both temperature and position and thus further analysis is needed. The processing includes eliminating questionable values, averaging the monthly values on a 2-deg grid, converting the means to anomalies (by subtracting the monthly climatological mean), interpolating missing values, applying a spatial median filter, replacing median values by original gridded values in regions with a high density of observations and, finally, smoothing linearly in space. (Complete details are given in appendix A.)

The most important step of the in situ analysis procedure is the application of the nonlinear filter based on medians which was developed by Tukey (see Rabiner et al., 1975) and which is applied spatially. The use of medians rather than weighted means results in the objective elimination of extreme values instead of smoothing the effect of the extremes over a larger region. The application of the filter (see appendix B for the algorithm) is made in several steps with different length scales of up to 8 deg and degrades the original 2-deg resolution to roughly 6 deg. The gridded values are filtered without regard to the number of observations that were used to compute the average. Since values obtained from a larger number of observations should be more accurate than those from a smaller number, the median filtered value was replaced in more dense reporting areas with the original gridded value. This technique enhances the gradients in some of the

*Corresponding author address:* Dr. Richard W. Reynolds, Climate Analysis Center/NMC/NWS/NOAA, WWB, Washington, DC 20233.

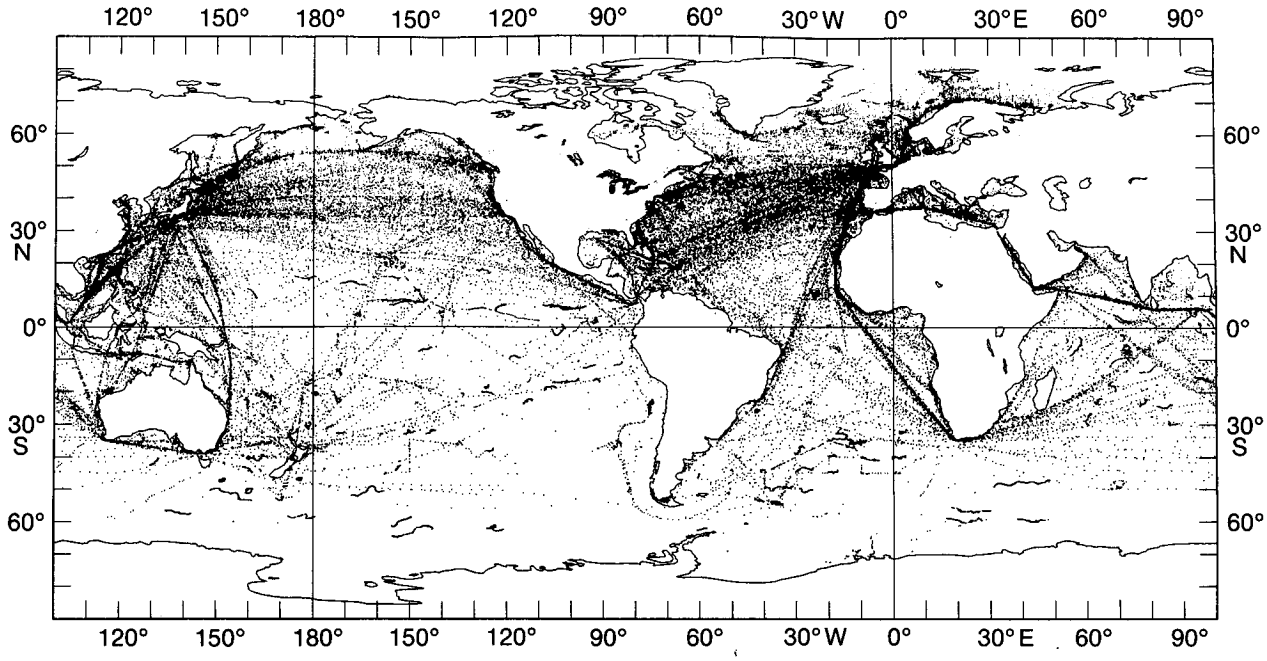


FIG. 1. Distribution of surface marine in situ (ship and buoy) observations received over the GTS for October 1986. (Drifting buoys may be distinguished as nearly continuous wiggly lines.)

better sampled coastal upwelling areas. An example of the in situ anomaly field after this processing is shown in Fig. 2.

### *b. The satellite analysis*

The use of satellite data can significantly improve the in situ analysis, especially in regions of sparse in situ data. At this time (see Njoku et al., 1985) the multichannel sea surface temperature (MCSST) technique of McClain et al. (1985), using the advanced very high resolution radiometer (AVHRR) on the NOAA polar orbiting satellites, is one of the more accurate SST retrieval methods. When comparing these measurements with conventional observations, it is important to note that the initial satellite measurement is a "skin" temperature (i.e., the temperature of a surface layer of less than a millimeter), while the in situ observations are "bulk" temperatures (i.e., the temperature of a surface layer on the order of meters). To correct for this difference, the satellite algorithms are "tuned" by regression against quality-controlled drifting buoy SST measurements. These regressions differ between day and night because different AVHRR channels are used. However, the regressions are not a function of global location or season.

The total number of MCSST satellite retrievals over the globe from 1982 through 1986 has varied from a low of two hundred thousand to over three million per month. This large variation is due to satellite hardware failures and to interpretation difficulties related to cloud cover and atmospheric aerosols. However, recent retrievals (see Fig. 3) have given excellent global monthly coverage.

The present NMC archive of MCSST retrievals is accessed daily. (Beginning in February 1985 the data were also separated into daytime and nighttime categories.) The analyzed field is computed using techniques similar to those used for the in situ analysis; the details are described in appendix C. However, because of the large number of observations, the median filtered value is replaced by the original gridded value in most regions. Thus, the most important step in the satellite procedure is a linear smoothing using a two-dimensional (1–2–1) binomial filter. The linear smoothing is needed for the later blending of the two analyses because (as discussed in subsection 2c) the first and second derivatives of the satellite field must be computed. An example of the resulting satellite anomaly field is shown in Fig. 4.

Because the global satellite coverage is superior to the in situ coverage, the satellite field has potentially better accuracy. This is demonstrated by the tendency of the Southern Hemisphere satellite anomalies to be more coherent in space and time than the in situ anomalies. However, direct comparisons of Figs. 2 and 4 show general similarities but with important differences of over 1°C (see Fig. 5) which occur even in northern midlatitude regions where the in situ coverage is also good. Figure 6 shows a monthly time series of the in situ and satellite analyses (1982–86) in two eastern Pacific regions: one in the tropics and one in northern midlatitudes. Generally, the satellite analysis is approximately 0.5°C colder than the in situ analysis.

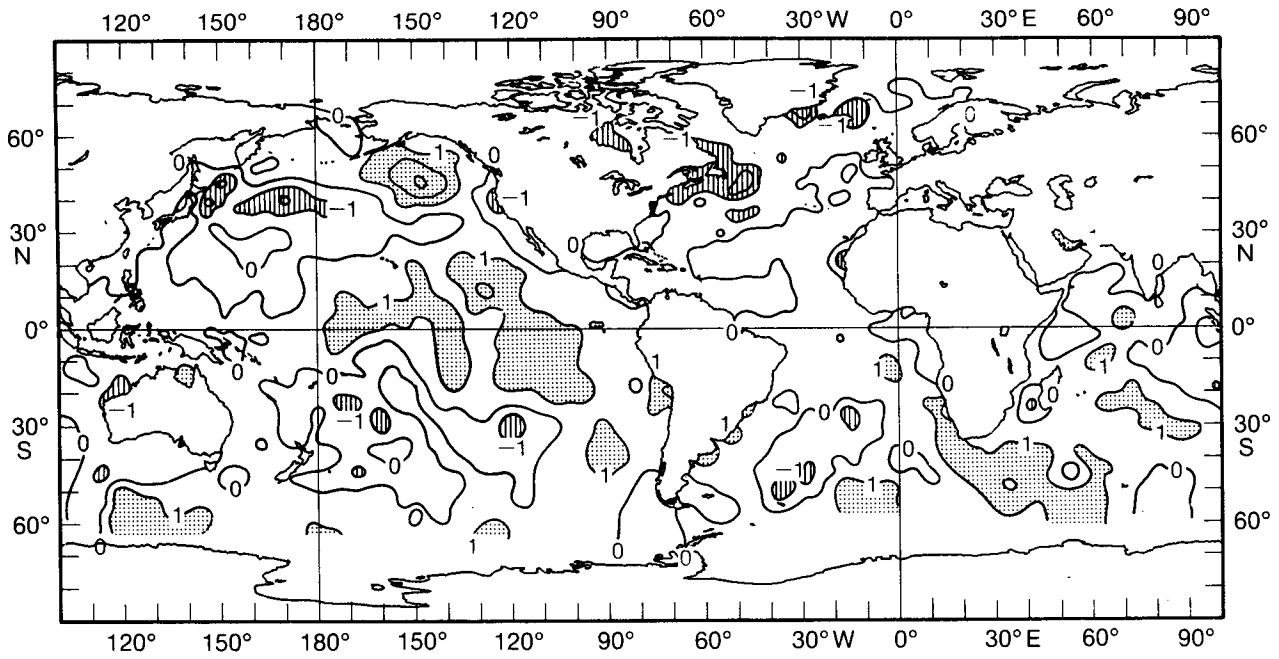


FIG. 2. Analyzed in situ SST anomaly field for October 1986. The contour interval is 1°C. Values less than −1°C are shaded; values greater than 1°C are stippled.

However, important reversals in these tendencies persist for several months. Both analyses clearly show the warming ENSO (El Niño/Southern Oscillation) signal of 1982–83 in the tropical Pacific.

These comparisons show that although SST information is found in both types of data, there are differences between them. Biases in ship intake temperatures have been well documented (e.g., see Barnett, 1984). (The biases are thought to be positive by several tenths of a degree Celsius although there is disagreement about

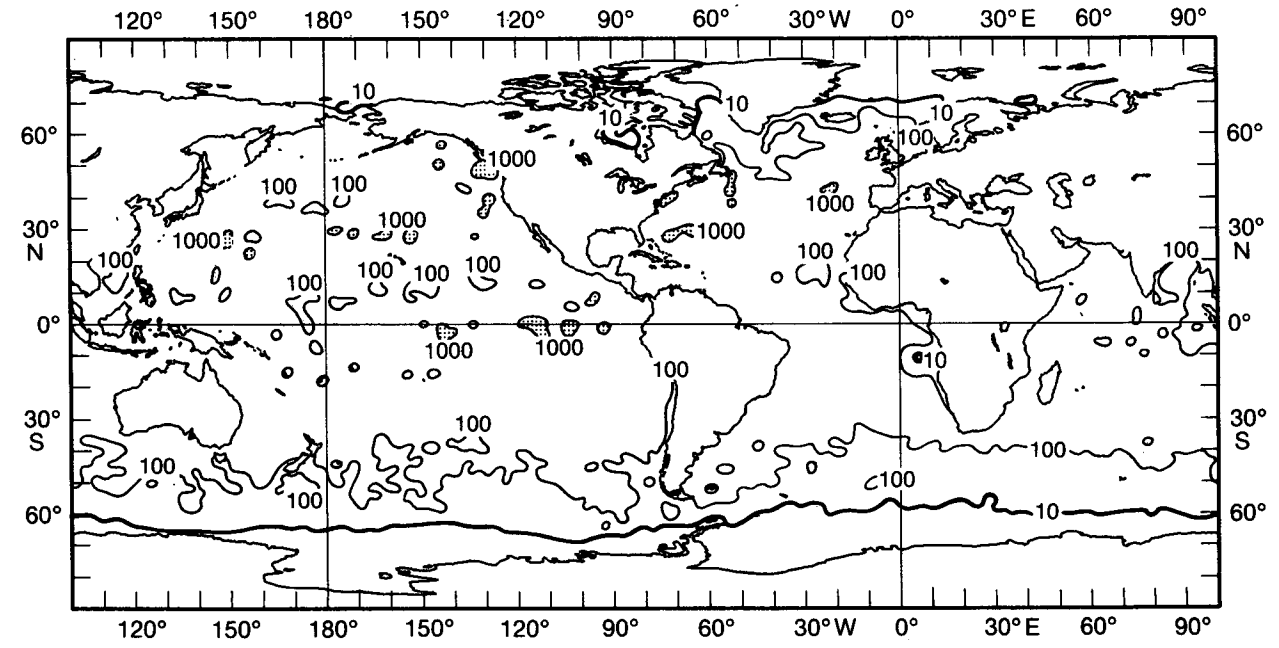


FIG. 3. Number of satellite (day plus night) observations available on a 2-deg grid for October 1986. The contours are 10 (heavy line), 100 and 1000. Values greater than 1000 are stippled.

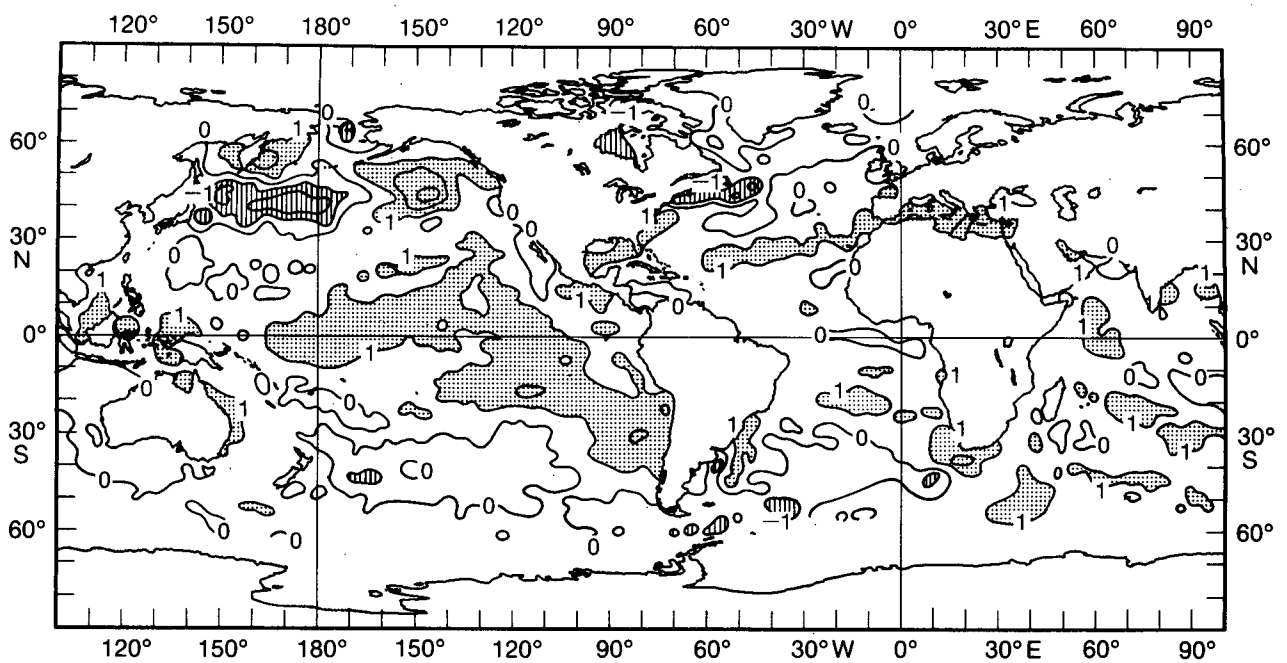


FIG. 4. As in Fig. 2 except for analyzed satellite SST anomaly field for October 1986.

the exact value.) However, satellite SST retrievals also have biases as discussed above. To illustrate the spatial scales of the satellite bias, monthly satellite fields were analyzed using only daytime or only nighttime observations. A typical difference (see Fig. 7) shows large coherent zonal regions where nighttime satellite temperatures were more than 0.5°C greater than daytime temperatures. Because this would be unlikely to occur in the open ocean for an entire month (especially in the tropics), biases in the satellite field may be inferred.

The causes of the satellite biases are only partially understood. Perhaps the best known example is the

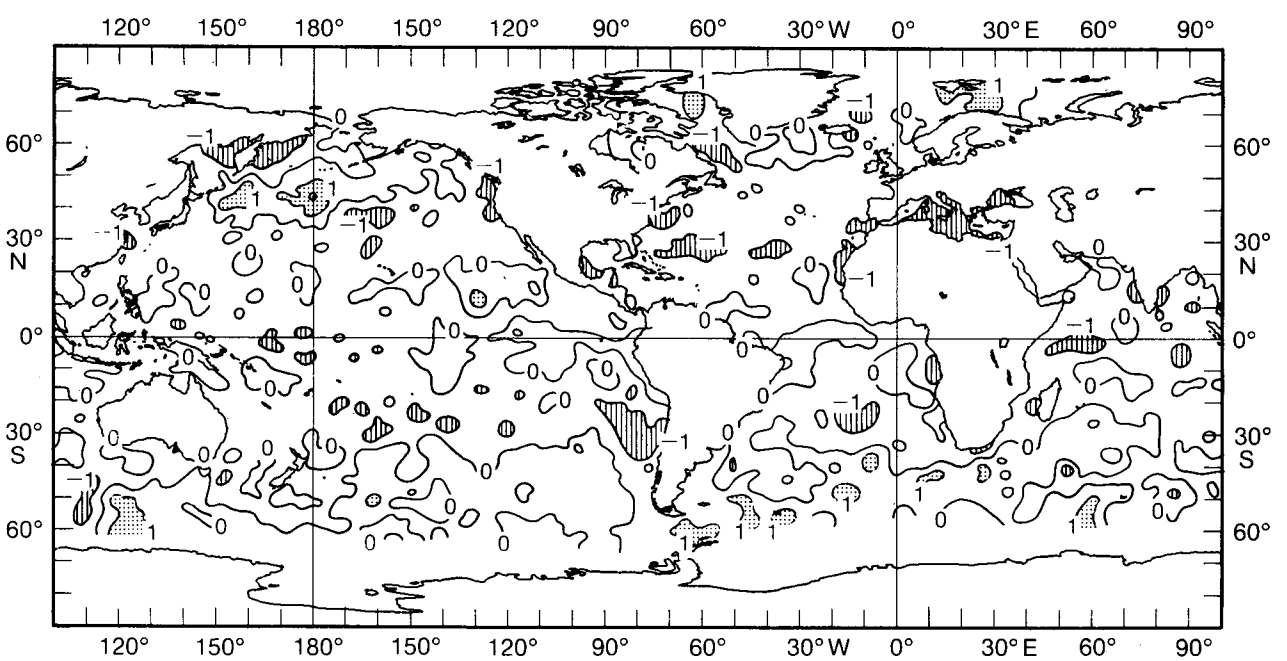


FIG. 5. As in Fig. 2 except for difference between in situ and satellite SST analyses (in situ − satellite) for October 1986.

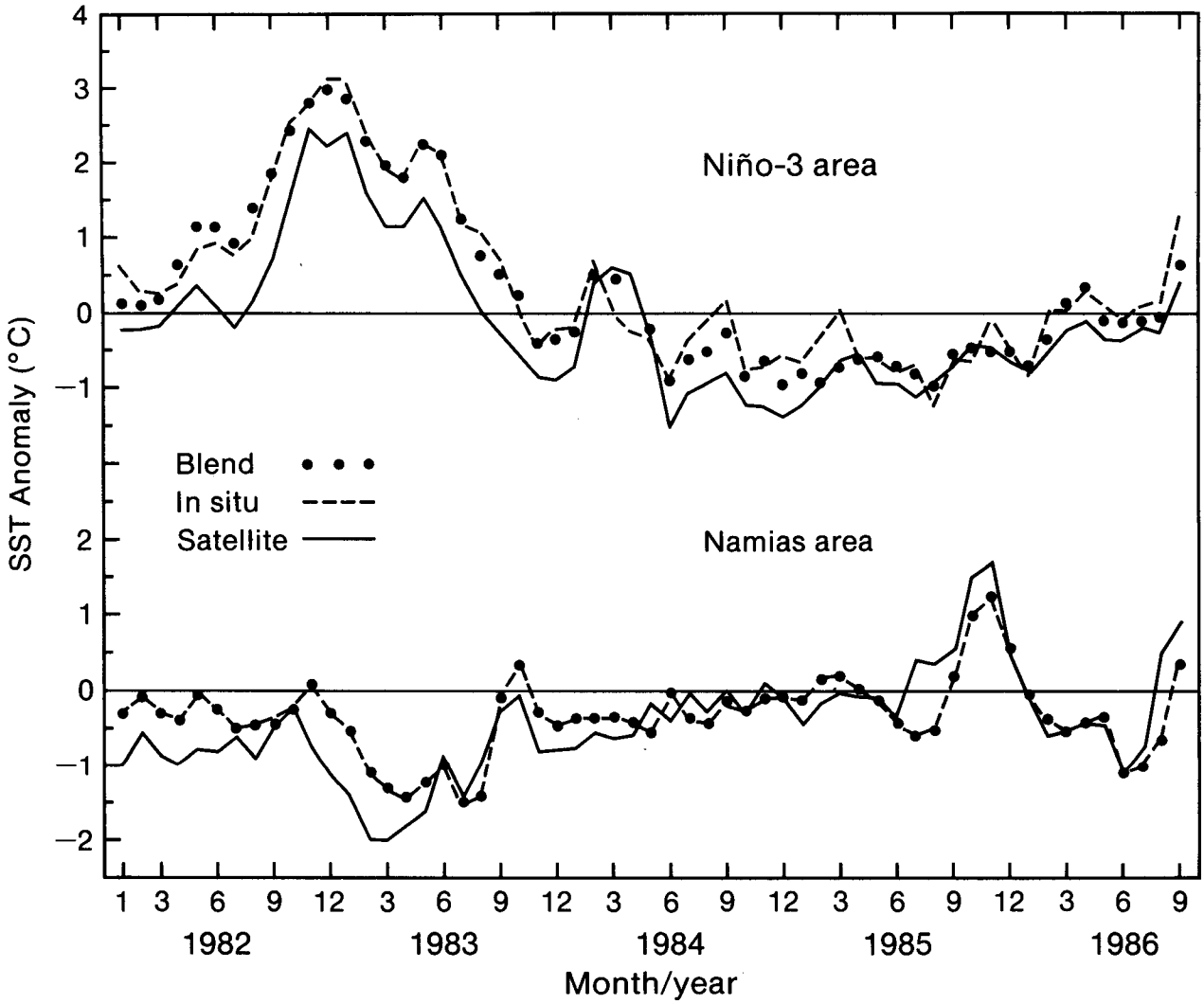


FIG. 6. Time series of in situ (dashed line) and satellite (solid line) SST anomalies for January 1982 to September 1986. The blended values (see text) are dotted. The Pacific regions are Niño 3 (5°S–5°N, 90°W–150°W) and Namias (30°N–50°S, 150°W–165°W).

SST biases which followed the March–April 1982 eruptions of El Chichón. The aerosols from the eruptions resulted in negative biases in the SST retrievals of over 2°C relative to the in situ reports (Strong, 1983). Within days after the eruptions, the aerosols (with the associated negative SST biases) were spread by the atmosphere along the latitude of the volcano, approximately 10°N. In the following months, they were gradually spread to other latitudes. (This can explain much of the satellite to in situ bias in 1982–83 in the tropical time series of Fig. 6 as well as the delayed bias in the midlatitude series.) Another source of negative bias occurs when cloud detection algorithms fail and the temperatures of cloud tops are mixed with SSTs. The causes of the biases are further complicated by the global "tuning" method which assumes that the relationship between "skin" and "bulk" temperatures are time and space independent. However, it is not the purpose of this work to explain satellite biases but only to identify that they exist. The analysis method which follows is designed to minimize their effects.

### *c. The blended analysis*

The method described in this section "blends" the two types of observations by using the in situ analysis to define "benchmark" temperature values in regions of frequent in situ observations and the satellite analysis to define the shape of the field in regions with little or no in situ data. This is done by requiring that the SST field satisfy Poisson's equation (see Oort and Rasmusson, 1971) in spherical coordinates. The blended field, $\phi$, is set equal to the in situ field at grid points where there are a sufficient number of in situ observations to define the analysis adequately. ("Sufficient" has been empirically defined—see below for more details—as

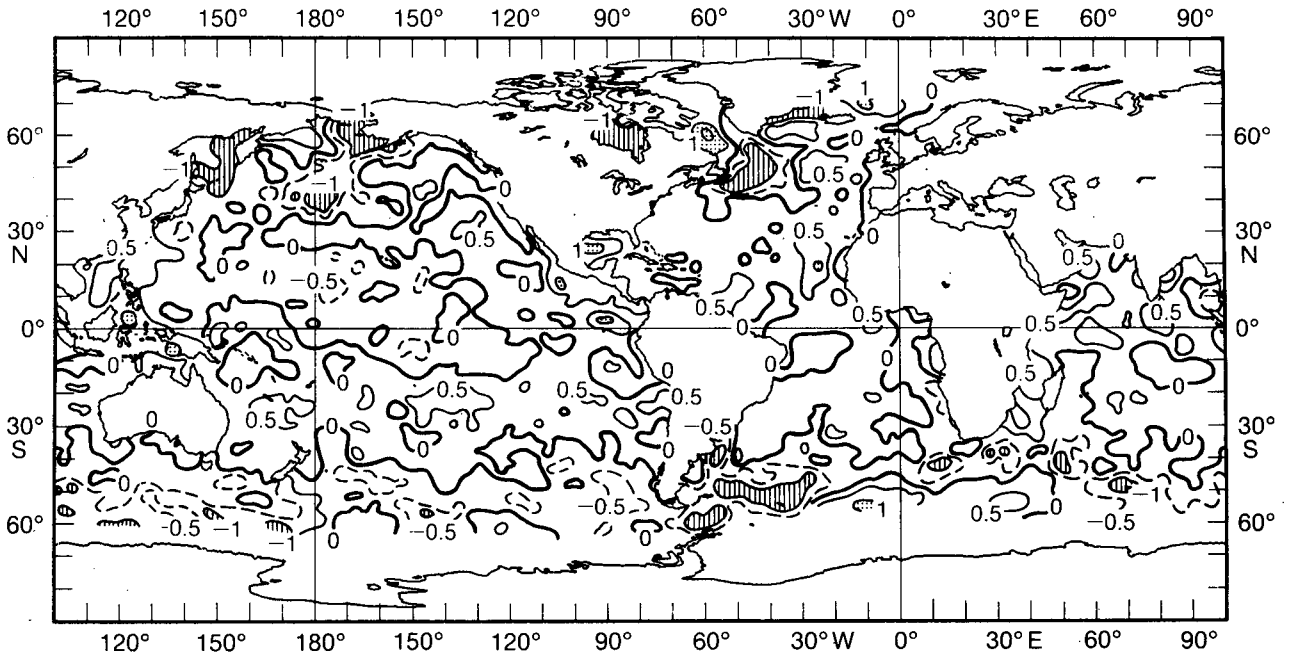


FIG. 7. Difference between satellite analyses using daytime or nighttime observations (day − night) for October 1986. Otherwise as in Fig. 2, except that the 0°C contour is indicated by a heavy line and additional contours are added at −0.5°C (dashed line) and 0.5°C (solid line).

five or more observations per grid box per month.) At the other grid points $\phi$ is determined by solving the equation

$$\nabla^2\phi = \rho, \tag{1}$$

subject to the internal boundary conditions imposed by the in situ benchmark values. The forcing term, $\rho$, is defined to be the Laplacian of the satellite analysis ($\nabla^2 S$) in regions of sufficient satellite observations (empirically defined—see below—to be ten or more observations per month) and 0 elsewhere. At grid points with less than ten satellite observations, therefore, the satellite field cannot locally affect the final result. At other grid points, the satellite field can only affect the solution via the Laplacian. Thus large-scale biases in the satellite field (i.e., biases with a Laplacian of zero) cannot affect the final solution in this aspect of the analysis.

To obtain a well-posed solution to (1), conditions must also be specified at an external boundary which completely encloses the interior region. This is done by initially defining the poleward limits of all SST measurements. At these limits $\phi$ is set equal to the in situ analysis, in regions of sufficient (five or more) in situ observations, or otherwise, set to the satellite analysis. Biases in the satellite data can thus enter the blended analysis when the external boundary conditions are derived from satellite observations. In this case the effects of the satellite biases spread toward lower latitudes where they are finally eliminated by in situ internal boundary points.

The technique involves two important choices which can only be defended empirically. The first choice requires that five or more in situ observations be available locally before a gridded value from the in situ analysis could be used as an internal or external boundary value. This criterion was selected experimentally and is a compromise between a blended field dominated by the satellite analysis (if more in situ data were required) or the in situ analysis (if less in situ data were required). The second choice was to set $\rho$ equal to the local Laplacian of the satellite analysis only if at least ten satellite observations had been available there; otherwise $\rho$ was set to 0. This criterion was selected after noting that the difference between in situ and satellite fields tended to be large when the number of monthly satellite retrievals per grid point became very low. The restriction is equivalent to linearly interpolating the satellite field across regions where the field is unreliable. It was tested during late 1982 when the effect of the El Chichón aerosols on the satellite retrievals produced an erroneous negative trough in the satellite anomaly field along 10°N. Because the trough was associated with a very low number of satellite retrievals, the ten-observation restriction allowed the trough to be automatically eliminated from the blend. However, during the more recent TOGA period, the restriction has minimal effect because of the limited number of interior ocean regions with less than ten satellite observations (e.g., see Fig. 3).

For computational convenience, the blended analysis is also computed for grid points on land. Since

there are no land observations, the solution automatically reduces to $\nabla^2\phi = 0$. However, along most of the coastal regions, the grid values become in situ internal boundary points because of the high density of ship traffic. This effectively isolates solutions on land from those on the sea.

The Poisson method was chosen primarily because it objectively eliminates both the bias and the large-scale gradient of the satellite field between the internal boundary points. This procedure allows the shape of the satellite field to be matched to the boundary points more effectively than by correction of the satellite bias alone. The Poisson equation also has the important benefit of behaving well numerically. Thus, when the equations are expanded by finite differences into a set of linear algebraic equations, they can be solved iteratively to obtain a unique solution. This behavior is especially convenient since the set of equations vary as the boundary points respond to changes in the monthly distribution of observations. The solution was done by sequential overrelaxation with a relaxation coefficient of 1.6 (e.g., see Thompson, 1961). For each complete iteration of all interior points, the solution was defined to have converged when the maximum absolute value of the individual grid point residuals was less than 0.001°C. The convergence took less than 300 iterations and was only weakly affected by the relaxation coefficient or by the convergence criterion. A final smoothing was done by a linear binomial (1–2–1) filter in both the north/south and east/west directions. An example of the blended field is shown in Fig. 8.

The effect of the blended procedure can be seen by examining the in situ, satellite and blended anomalies (Figs. 2, 4 and 8) as well as the difference between the in situ and the blended fields (Fig. 9) and the satellite and the blended fields (Fig. 10). These figures show that the satellite analysis has almost no effect on the blend from approximately 60°N to the equator in the Atlantic and Indian oceans and from approximately 55° to 20°N in the Pacific Ocean. In these regions the in situ data are sufficiently dense so that almost all of the grid values become internal boundary values. In the remaining areas the blended field is a mix of the two input analyses so that the blend retains the average anomaly value from the in situ field with the greater coherence of the satellite field. (The change in the coherence is evident by the smoothness contrast between Figs. 9 and 10.) To illustrate the behavior of the blend with time, the blended anomalies have been included in the time series of Fig. 6. In the midlatitude series the in situ and blend are almost identical due to the large number of internal in situ boundary points. However in the tropical time series, where the in situ data are more sparse, the blend uses the in situ field as a reference in spite of changing satellite biases.

### *d. SST climatology*

The monthly SST climatology of Reynolds and Roberts (1987) has been used in the SST analyses. Although complete details of the processing can be found there, a summary is included here.

An initial climatological monthly analysis was completed using the in situ data from the Comprehensive

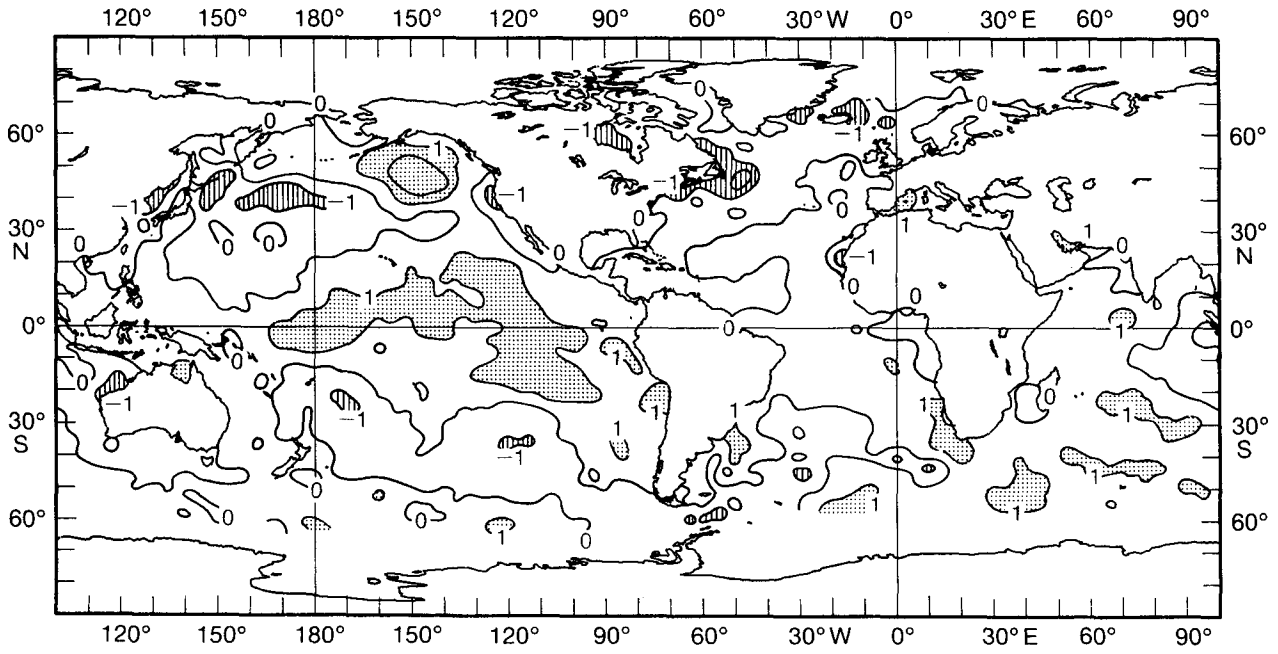


FIG. 8. As in Fig. 2 except for analyzed blended SST anomaly for October 1986.

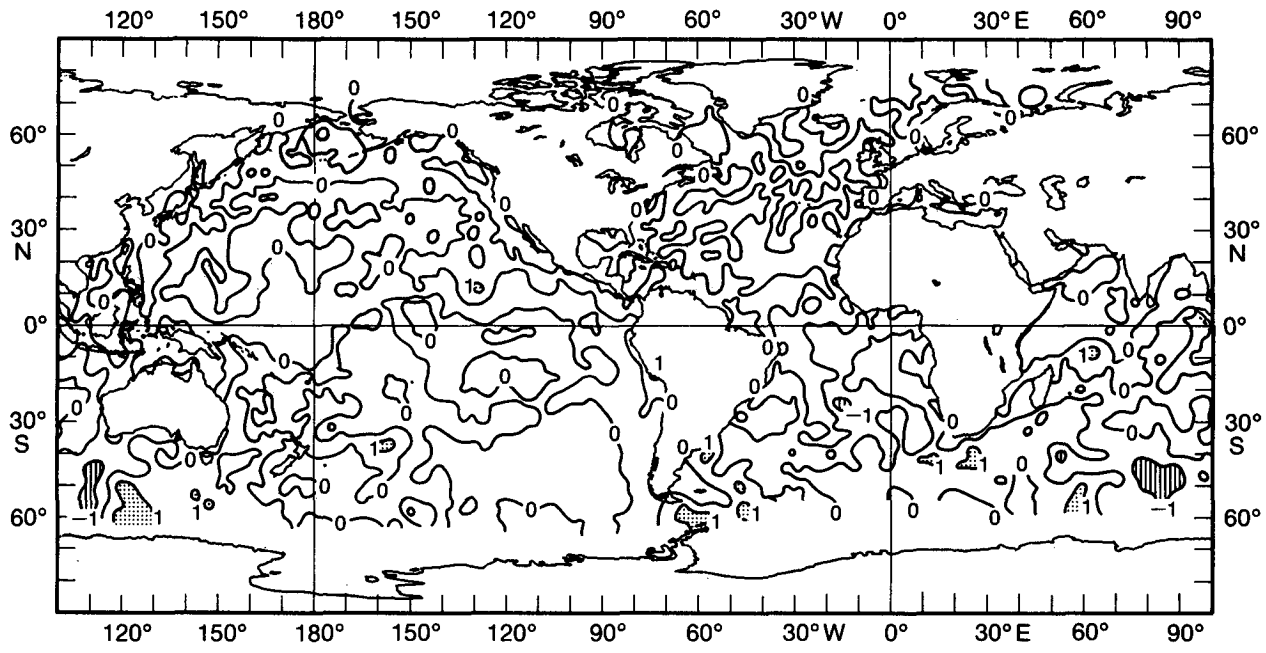


FIG. 9. As in Fig. 2 except for difference between in situ and blended SST analyses (in situ − blend) for October 1986.

Ocean–Atmosphere Data Set (COADS) of Slutz et al. (1985) for the period 1950–79. This was done by first combining all data for the same month, without regard for year, on a 2-deg grid. Then following a median filter procedure similar to that of the in situ analysis above, monthly climatological fields were obtained. However, because of the lack of data in the Southern Hemisphere, the climatological fields were extended using ice and satellite data. The ice data (obtained from a 10-yr dataset from the Glaciological Data Center, Boulder, Colorado) were used to produce monthly fields which indicate the percentage of time that each

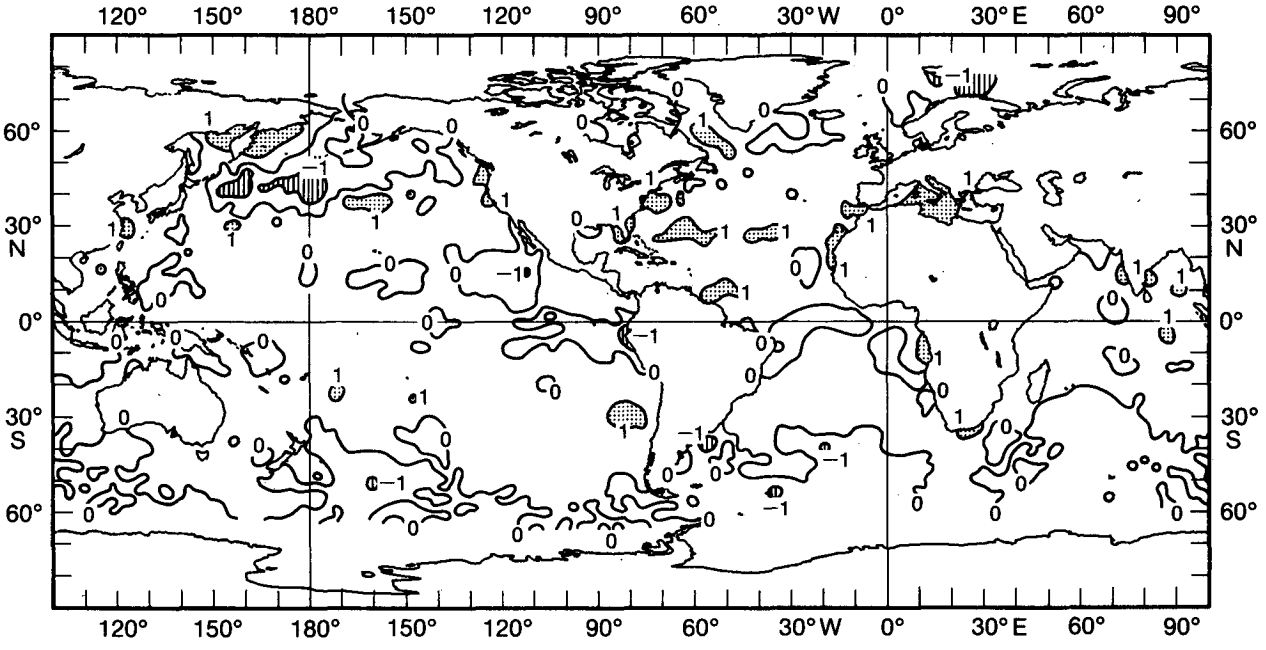


FIG. 10. As in Fig. 2 except for difference between satellite and blended SST analyses (satellite − blend) for October 1986.

grid point was covered by ice during the 10 years. If sea ice was present at least 50% of the time, the monthly climatological SST at that point was set equal to −1.8°C, the freezing point of seawater at a salinity of 35 ppt. (A similar procedure was used by Alexander and Mobley, 1976.) At the non-ice grid points, the monthly SST climatology was set equal to the preliminary COADS in situ analysis if at least ten observations had been available there. In the remaining interior regions, the grid points were found by solving (1) where the forcing term was determined by a monthly satellite climatology. The satellite climatology was computed by averaging 4 yr (1982–85) of the monthly satellite analyses described above. The effect of satellite SST biases was minimal in the climatology since the satellite analysis was only used to determine the shape of the solution in internal regions of the field and was not used to define external boundary conditions as in the operational procedure described above.

## 3. Verification

In this section, quality-controlled drifting buoy data are used to provide objective error statistics for all three analyses during the first 2 years of the TOGA period. The quality-control procedure (see appendix A for complete details) only accepts buoy data which pass certain tests on the SST measurements themselves and on the buoy speed and position. The error statistics are calculated by first computing a monthly averaged temperature (and position) for each quality-controlled buoy and comparing it to a value at the same location which was obtained by interpolation from all three of the monthly analyzed SST fields. (Although some buoys move distances of 1000 km or more in a month, the SST changes are relatively small because the buoys tend to drift with water of the same physical characteristics.) To ensure that the verifying analyses are as independent of the buoys as possible, special versions of the in situ and the blended analyses were computed by withholding the drifting buoy data. The satellite analysis, and therefore the verifying version of the blend, are not completely independent of the buoy observations since the satellite algorithms are "tuned" at 6- to 12-month intervals by regression against the drifting buoy data. (This "tuning" is done aperiodically when new satellites are made operational or when errors between the satellite retrievals and the buoy temperatures suggest that the satellite calibrations may have changed.)

Monthly biases and rms errors between the quality-controlled buoy data and the satellite and the special in situ and blended analyses have been computed for all 24 months from January 1985 to December 1986. The results (abbreviated in Table 1) show that the modulus of the monthly buoy-to-analysis biases (i.e., the average of the absolute value of the monthly biases) varies from 0.09° to 0.15°C. The table indicates that the modulus of the buoy to blend bias is slightly better than the others. The average rms buoy to analysis error varies from 0.78° to 1.09°C. In contrast to the modulus, the rms buoy to analysis error is the smallest for the satellite analysis although the blended analysis is very similar. In both cases the buoy to in situ analysis has the worst modulus of the bias and the worst rms error, primarily because of the lack of high latitude Southern Hemisphere ship data which, in turn, results in an ill-defined SST field there. The buoy distribution (see Fig. 1) is not uniform over the globe since it was designed to complement other in situ data. (During this 2-yr period more than two-thirds of the buoys were located in the Southern Hemisphere.)

The tropical Pacific, especially its western portion, is a region where the accuracies of the SSTs are of particular concern for diagnosing and predicting ENSO phenomena. Therefore, statistics comparing the analyses to drifting buoys were examined for the Pacific between 20°N and 20°S. In this case the average rms error for all analyses reduced to less than 0.5°C. This error is less than the globally averaged error because of the contribution to the latter from large differences between the buoys and the analyses in higher latitudes near strong oceanographic fronts. However, since the number of buoys in the tropical Pacific was as low as six per month, the rms statistics there should be used with caution.

## 4. Concluding remarks

Details have been presented of an SST analysis which blends both in situ and satellite data. The method uses preliminary in situ and satellite analyses as input fields. The in situ analysis is used as ground truth to provide "benchmark" temperatures in regions of frequent in situ observations; the satellite analysis is used to define the shape of the final field between the benchmarks. Examples have been presented which suggest that the blended technique is an effective way to utilize the improved satellite coverage while eliminating much of the bias between in situ and satellite data.

Comparisons using drifting buoy data showed that the modulus of the buoy to blend monthly biases was less than 0.1°C while the average rms buoy to blend error was less than 0.8°C. Although these results indicated that the blend was an improvement over the in situ analysis, they did not clearly indicate that the blend was superior to the satellite analysis. This result may seem surprising when contrasted with the satellite to in situ biases (e.g. see Fig. 6) which have been discussed earlier. Further comparisons using additional SST analyses and additional SSTs from bathythermographs are now being completed in a cooperative effort with the United Kingdom Meteorological Office and will soon be ready for publication. The statistical results show that the satellite biases are nonzero at the 5% significance level. The reason that the drifting buoy data cannot strongly distinguish whether the satellite

TABLE 1. Global bias and rms statistics between monthly SST analyses and monthly averaged SST from quality-controlled drifting buoys for January 1985 through December 1986. The bias is defined as (buoy − analysis); only every third month is shown.

| Month | Year | Number of drifting buoys | Type of comparison | Bias (°C) | rms (°C) |
|---|---|---|---|---|---|
| January | 1985 | 59 | in situ | .04 | 0.97 |
| | | | satellite | .01 | 0.74 |
| | | | blend | .01 | 0.87 |
| April | 1985 | 84 | in situ | −.17 | 1.01 |
| | | | satellite | −.15 | 0.58 |
| | | | blend | −.02 | 0.72 |
| July | 1985 | 77 | in situ | −.23 | 1.07 |
| | | | satellite | −.13 | 0.63 |
| | | | blend | .00 | 0.81 |
| October | 1985 | 79 | in situ | −.30 | 1.34 |
| | | | satellite | −.26 | 0.97 |
| | | | blend | −.14 | 1.00 |
| January | 1986 | 101 | in situ | −.15 | 0.85 |
| | | | satellite | −.29 | 0.63 |
| | | | blend | −.16 | 0.61 |
| April | 1986 | 135 | in situ | −.02 | 0.83 |
| | | | satellite | −.05 | 0.72 |
| | | | blend | .02 | 0.71 |
| July | 1986 | 123 | in situ | −.17 | 1.13 |
| | | | satellite | .04 | 0.81 |
| | | | blend | .01 | 0.81 |
| October | 1986 | 110 | in situ | .03 | 1.05 |
| | | | satellite | −.18 | 0.99 |
| | | | blend | −.04 | 1.01 |
| Average (24 months) | | 99 | in situ | −.13 | 1.09 |
| | | | satellite | −.09 | 0.74 |
| | | | blend | −.01 | 0.78 |
| Modulus (24 months) | | 99 | in situ | .15 | — |
| | | | satellite | .12 | — |
| | | | blend | .09 | — |

or the blended analysis is superior is almost certainly due to their use in the aperiodic "tuning" of the satellite algorithms.

The blended analysis is a continuing effort to obtain the best real-time SST fields for the TOGA period (1985–94). Each blended field is carefully monitored each month using the drifting buoy data and the in situ and satellite analyses as diagnostic tools. The analysis may be modified in the future when the accuracy of the technique can be improved or when required by changes in the available observations.

*Acknowledgments.* I am grateful to E. Rasmusson for the encouragement to begin this work. I would also like to thank W. Gemmill, M. Halpert, C. Nelson, and L. Roberts for their computer expertise. M. Bottomley, C. Folland, W. Gemmill, R. Legeckis, and D. Parker provided helpful criticism in early drafts of this paper. I also wish to thank the editor, R. Rosen, and his reviewers for their help in improving the final version.

## APPENDIX A

### In Situ Analysis Procedure

The in situ analyzed field is computed as follows:

1) All drifting buoy observations are separated from the other in situ data and sorted by buoy identification. (This is done because the drifting buoy data have a high frequency of real time observations in regions which may have little other in situ observations.) Monthly time series of buoy position, speed, and SST are produced and smoothed with a five-point temporal median filter to eliminate some spikes in the data. If one of the time series for a buoy fails any of the following gross error tests, *all* data for the buoy are rejected for the month.

(a) Tests on each monthly time series of buoy position are:

(i) Any absolute change in position between adjacent points is greater than 3° lat or 3° long.
(ii) The buoy position does not change during the month.
(iii) The monthly standard deviation of position is greater than 10° lat or 10° long.
(iv) The buoy is located over land.

(b) Tests on each monthly time series of buoy speed are:

(i) Any individual buoy speed is greater than 5 m/s.
(ii) The monthly standard deviation of speed is greater than 3 m/s.

(c) Tests on each monthly time series of buoy SST are:

(i) Any absolute change in SST between adjacent points is greater than 5°C.
(ii) The buoy SST does not change.
(iii) The monthly standard deviation of SST is greater than 4°C.
(iv) The monthly mean SST is not within four standard deviations of the monthly climatological SST.

2) The individual observations from fixed buoys or ships are discarded if they are located over land or if they differ from the local climatological mean by more than four standard deviations.

3) All the remaining in situ observations for the month (approximately 100 000) are used to compute an initial gridded field by arithmetically averaging the observations within a 2-deg lat and long (centered on even values). The gridded values are then converted to anomalies by subtracting the climatological monthly mean.

4) Monthly grid point SST values are then discarded if they fail any of the following screening tests:

(a) The absolute value of the anomaly is greater than 8°C.
(b) The absolute value of the anomaly is greater than 6°C, the number of observations is 2, and the location is either north of 60°N or south of 30°S.
(c) The absolute value of the anomaly is greater than 3°C, the number of observations is 1, and the location is either north of 60°N or south of 30°S.
(d) The number of observations is 1 and there are no observations in any of the four neighboring boxes to the north, south, east, or west.
(e) The magnitude of the difference between the gridded 2-deg anomaly value and the nearest grid point in a separate analysis of the anomaly field on a coarser grid was more than 4°C. (This test was designed to eliminate gridded values which disagreed strongly with their neighbors. The separate analysis was completed on a 4-deg lat and long grid using all the steps in this procedure except this one. The new analysis, although smoothed, should be accurate enough to allow any original 2-deg gridded value to be eliminated if it differed greatly from the smoothed field. Since anomalies were used throughout, the effect on strong gradient regions, e.g., western boundary currents, was minimal.)

5) All grid points without an assigned value (i.e., either no observations were available or the grid value was discarded) are filled by interpolation or extrapolation using an objective analysis based on the iterative difference-successive correction method of Cressman (1959).

6) The spatial median filter (described in the main text and appendix B) is applied.

7) The median filtered value is replaced by the original arithmetically averaged value for all grid points having at least 30 observations. For grid points with 15 to 30 observations, a linear combination of the filtered and original values is used so that there is no effect on the median filtered value for 15 observations, but there is total replacement by the original value for 30 observations.

8) A final linear smoothing using a binomial (1–2–1) filter in both the north/south and east/west direction is applied.

As described in section 2, the median filter (step 6) is the most important step in the in situ analysis. The data screening (step 4) is designed to eliminate questionable observations in regions of sparse data. If these observations are not eliminated, their effects are spread over larger regions by the filling of missing data (step 5). If such regions exceed the maximum spatial width of the median filter (eight degrees), they are unaffected by the filtering and remain in the final product. The replacement procedure (step 7) permits grid values with a large number of observations to have a greater influence on the analyzed field. This enhances the gradients in some of the well-sampled coastal upwelling regions. The linear filter (step 8) smoothes the field to produce the final in situ field.

## APPENDIX B

## Median Filter Algorithm

The median filter was obtained from unpublished notes by John Tukey (see Rabiner et al., 1975, for a general discussion). Given a time series of $n$ data points $z_i$ where $i = 1, 2, \cdots, n$, the filter function $f(z_i)$ is defined as follows:

$$y_{i+3/2} = \text{median}(z_i, z_{i+1}, z_{i+2}, z_{i+3}) \quad \text{for} \quad i = 1, 2, \cdots, n-3,$$

$$x_{i+3/2} = \text{median}(y_{i+1/2}, y_{i+3/2}, y_{i+5/2}) \quad \text{for} \quad i = 2, 3, \cdots, n-4,$$

$$v_{i+1} = \text{median}(x_{i+1/2}, x_{i+3/2}) \quad \text{for} \quad i = 3, 4, \cdots, n-4,$$

and

$$f(z_{i+1}) = \text{median}(v_i, v_{i+1}, v_{i+2}) \quad \text{for} \quad i = 4, 5, \cdots, n-5.$$

To filter the data, the function is applied twice. The first use defines a change in $z_i$, $\Delta z_i$, as

$$\Delta z_i = z_i - f(z_i) \quad \text{for} \quad i = 5, 6, \cdots, n-4,$$

and

$$\Delta z_i = 0 \quad \text{for} \quad i = 1, 2, 3, 4 \quad \text{and} \quad i = n-3, n-2, n-1, n.$$

The second gives the final filtered series $u_i$ as

$$u_i = f(z_i) + f(\Delta z_i) \quad \text{for} \quad i = 5, 6, \cdots, n-4.$$

In this paper the filter was applied spatially, first in the east/west and then in the north/south direction. Since the filter was undefined at the end of each spatial series, the length of each series was increased by adding ten points to both ends. In the east/west direction the spatial series then overlapped along latitudinal circles. The extra values needed in this direction were obtained by repeating values in a cyclic manner. The extra values in the north/south direction were obtained by repeating the original first and last values at the beginning and end of the series, respectively.

## APPENDIX C

### Satellite Analysis Procedure

The satellite SST analysis is computed as follows.

1) All satellite SST observations for the month (both day and night) are arithmetically averaged on a 2-deg lat and long grid and converted to anomalies by subtracting the climatological monthly mean.

2) Grid point SST values are then discarded if they fail any of the following screening tests:

(a) The absolute value of the anomaly is greater than 8°C.

(b) The absolute value of the anomaly is greater than 5°C and the number of observations is less than 30.

(c) The absolute value of the anomaly is greater than 2°C and the number of observations is less than 10.

(d) The number of observations is 3 or less.

(e) The magnitude of the difference between the gridded 2-deg anomaly value and the nearest grid point in a separate analysis of the anomaly field on a coarser 4-deg grid was more than 4°C. (As in the in situ analysis, this test was designed to eliminate gridded values which disagreed strongly with their neighbors.)

3) All grid points without an assigned value (i.e., either no observations were available or the grid value was discarded) are filled by interpolation or extrapolation using an objective analysis scheme based on the iterative difference-successive correction method of Cressman (1959).

4) The spatial median filter is applied.

5) The median filtered value is replaced by the original arithmetically averaged for all grid points having at least 100 observations. For grid points boxes with 30 to 100 observations, a linear combination of the filtered and original values is used so that there is no effect on the median filtered value for 30 observations but there is total replacement by the value for 100 observations. (The number of observations for replacement are higher for the satellite analysis than for the in situ analysis because the satellite observations were made from one instrument while the in situ observations were made from different instruments with assumed independence of observational errors.)

6) A final linear smoothing using a binomial (1–2–1) filter in both the north/south and east/west directions is applied.

In spite of the similarity with the in situ analysis, the effect of the median filter is small in the satellite analysis because the number of satellite observations results in the replacement (step 5) of approximately 70% of the median values by the original arithmetically averaged values. Because of the replacement, the final linear smoothing (step 6) has the most influence on the final satellite field.

## REFERENCES

Alexander, R. C., and R. L. Mobley, 1976: Monthly average sea surface temperature and ice-pack limits on a 1° global grid. *Mon. Wea. Rev.*, **104,** 143–148.

Barnett, T. P., 1984: Long-term trends in sea surface temperatures over the ocean. *Mon. Wea. Rev.*, **112,** 303–313.

Cressman, G. P., 1959: An operational objective analysis system. *Mon. Wea. Rev.*, **87,** 367–374.

McClain, E. P., W. G. Pichel and C. C. Walton, 1985: Comparative performance of AVHRR-based multichannel sea surface temperature. *J. Geophys. Res.*, **90,** 11 587–11 601.

Njoku, E. G., T. P. Barnett, R. M. Laurs and A. C. Vastano, 1985: Advances in satellite sea surface temperature measurements and oceanographic applications. *J. Geophys. Res.*, **90,** 11 573–11 586.

Oort, A. H., and E. M. Rasmusson, 1971: Atmospheric Circulation Statistics. NOAA Professional Paper No. 5, 323 pp. [Available from US Government Printing Office, Washington, DC, 20402, Stock No. 0317-0045.]

Rabiner, L. R., M. R. Sambar and C. E. Schmidt, 1975: Applications of nonlinear smoothing algorithm to speech processing. *IEEE Trans. on Acoust. Speech Signal Process,* **ASSP-23,** 552–557. [Available from IEEE, 345 East 47 Street, New York, NY 10017.]

Reynolds, R. W., and L. Roberts, 1987: A global sea surface temperature climatology from in situ, satellite and ice data. *Trop. Ocean–Atmos. Newslett.*, **37,** 15–17. [Available from Rosentiel School of Marine and Atmospheric Science, 4600 Rickenbacker Causeway, Miami, FL 33149.]

Slutz, R. J., S. J. Lubker, J. D. Hiscox, S. D. Woodruff, R. L. Jenne, D. H. Joseph, P. M. Steurer and J. D. Elms, 1985: *COADS, Comprehensive Ocean–Atmosphere Data Set.* Release 1, 262 pp. [Available from Climate Research Program, Environmental Research Laboratories, 325 Broadway, Boulder, CO 80303.]

Strong, A. E., 1983: Satellite-derived sea surface temperature errors due to El Chichón aerosol cloud. *Trop. Ocean–Atmos. Newslett.*, **18,** 14–15. [Available from Rosentiel School of Marine and Atmospheric Science, 4600 Rickenbacker Causeway, Miami, FL 33149.]

Thompson, P. D., 1961: *Numerical Weather Analysis and Prediction.* The Macmillan Co., 170 pp.